

Boise State University  
**ScholarWorks**

---

Materials Science and Engineering Faculty  
Publications and Presentations

Department of Materials Science and  
Engineering

---

9-12-2016

## High-Performance and Flexible Thermoelectric Films by Screen Printing Solution-Processed Nanoplate Crystals

Tony Varghese  
*Boise State University*

Courtney Hollar  
*Boise State University*, [courtneyhollar@boisestate.edu](mailto:courtneyhollar@boisestate.edu)

Joseph Richardson  
*Boise State University*

Nicholas Kempf  
*Boise State University*

Chao Han  
*Boise State University*

*See next page for additional authors*

Follow this and additional works at: [https://scholarworks.boisestate.edu/mse\\_facpubs](https://scholarworks.boisestate.edu/mse_facpubs)

 Part of the [Materials Science and Engineering Commons](#)

---

### Publication Information

Varghese, Tony; Hollar, Courtney; Richardson, Joseph; Kempf, Nicholas; Han, Chao; Gamarachchi, Pasindu; Estrada, David; and Zhang, Yanliang. (2016). "High-Performance and Flexible Thermoelectric Films by Screen Printing Solution-Processed Nanoplate Crystals". *Scientific Reports*, 6, 33135-1 - 33135-6. <https://dx.doi.org/10.1038/srep33135>


For a complete list of authors, please see article.

---

**Authors**

Tony Varghese, Courtney Hollar, Joseph Richardson, Nicholas Kempf, Chao Han, Pasindu Gamarachchi, David Estrada, and Yanliang Zhang

# SCIENTIFIC REPORTS



OPEN

## High-performance and flexible thermoelectric films by screen printing solution-processed nanoplate crystals

Tony Varghese<sup>1</sup>, Courtney Hollar<sup>2</sup>, Joseph Richardson<sup>3</sup>, Nicholas Kempf<sup>2</sup>, Chao Han<sup>2</sup>, Pasindu Gamarachchi<sup>2</sup>, David Estrada<sup>1</sup>, Rutvik J. Mehta<sup>4</sup> & Yanliang Zhang<sup>1,2</sup>

Received: 27 May 2016

Accepted: 22 August 2016

Published: 12 September 2016

Screen printing allows for direct conversion of thermoelectric nanocrystals into flexible energy harvesters and coolers. However, obtaining flexible thermoelectric materials with high figure of merit ZT through printing is an exacting challenge due to the difficulties to synthesize high-performance thermoelectric inks and the poor density and electrical conductivity of the printed films. Here, we demonstrate high-performance flexible films and devices by screen printing bismuth telluride based nanocrystal inks synthesized using a microwave-stimulated wet-chemical method. Thermoelectric films of several tens of microns thickness were screen printed onto a flexible polyimide substrate followed by cold compaction and sintering. The n-type films demonstrate a peak ZT of 0.43 along with superior flexibility, which is among the highest reported ZT values in flexible thermoelectric materials. A flexible thermoelectric device fabricated using the printed films produces a high power density of 4.1 mW/cm<sup>2</sup> with 60 °C temperature difference between the hot side and cold side. The highly scalable and low cost process to fabricate flexible thermoelectric materials and devices demonstrated here opens up many opportunities to transform thermoelectric energy harvesting and cooling applications.

Thermoelectric conversion is a solid-state and environmentally friendly energy conversion technology with broad applications including solid-state cooling, energy harvesting, and waste heat recovery<sup>1</sup>. Flexible thermoelectric devices are especially attractive for waste heat recovery along contoured surfaces and for energy harvesting applications to power sensors, biomedical devices, and wearable electronics – an area under exponential growth<sup>2</sup>.

The efficiency of thermoelectric materials is determined by the figure of merit ZT defined as  $ZT = \alpha^2 \sigma T / \kappa$ , where  $\alpha$ ,  $\sigma$ ,  $\kappa$  and  $T$  are the Seebeck coefficient, electrical conductivity, thermal conductivity, and absolute temperature respectively<sup>3,4</sup>. Nanostructured thermoelectric materials have been widely studied in recent years and proven to have unique and superior thermoelectric performance compared to their bulk counterparts due to the ability to tailor electron and phonon transport and effectively increase ZT<sup>5–7</sup>. Despite significant ZT improvements in nanostructured materials<sup>8–10</sup>, the lack of scalable and low-cost manufacturing processes remains a major challenge to the wide use of these materials<sup>11</sup>. In addition, major progress in ZT enhancement through nanostructuring has historically been achieved in mechanically rigid materials, while flexible thermoelectric materials are still relatively unexplored and have fairly low ZT<sup>2</sup>.

Among all the methods to fabricate thermoelectric materials, wet deposition of nanocrystal-based colloidal inks using screen printing, inkjet printing, direct writing, or other layer-by-layer methods hold many advantages due to the ability to directly convert nanocrystal inks into micro/macroscale functional materials and devices with great scalability, flexibility, and cost effectiveness<sup>12,13</sup>. Using inkjet or disperser printing, several research groups have achieved ZT of ~0.3 in thermoelectric films printed on flexible substrates<sup>14,15</sup>. Screen printing has also been explored as a more efficient way to fabricate thermoelectric devices<sup>16–19</sup>. Despite the above proof-of-concept demonstrations, flexible thermoelectric films fabricated by printing methods continue to exhibit fairly low ZT in

<sup>1</sup>Micron School of Materials Science and Engineering, Boise State University, Boise, ID 83725, United States.

<sup>2</sup>Department of Mechanical and Biomedical Engineering, Boise State University, Boise, ID 83725, United States.

<sup>3</sup>Department of Electrical and Computer Engineering, Boise State University, Boise, ID 83725, United States.

<sup>4</sup>ThermoAura Inc. 132 B. Railroad Avenue, Colonie, NY 12205, United States. Correspondence and requests for materials should be addressed to Y.Z. (email: yanliangzhang@boisestate.edu)

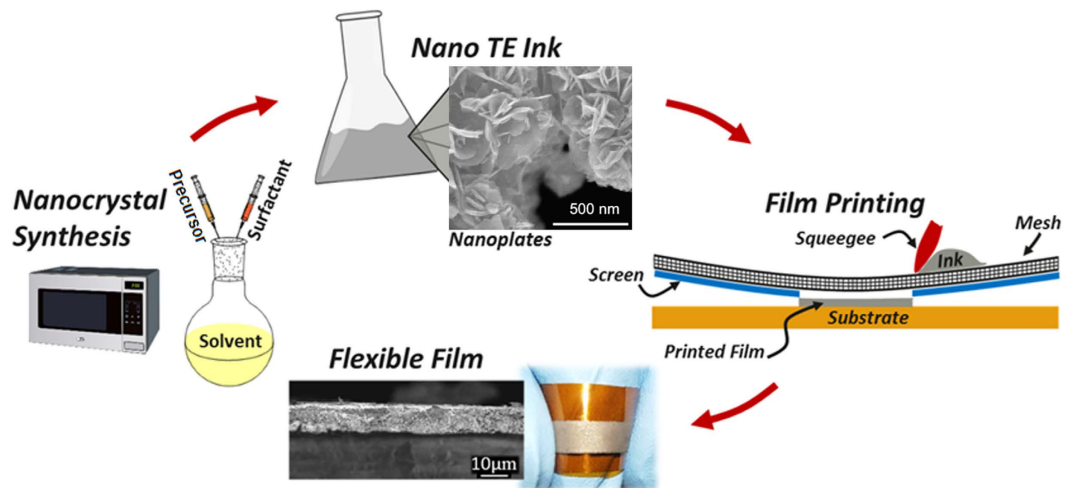


**Figure 1.** Schematic illustration of overall fabrication process for the flexible thermoelectric films, including nanocrystal synthesis, nano-ink processing, screen printing of thermoelectric films on flexible substrate, and sintered flexible films.

the 0.1–0.3 range, significantly lower than their rigid bulk counterparts fabricated using conventional approaches such as hot press or spark plasma sintering<sup>2</sup>. There are many challenges in printing efficient and flexible thermoelectric materials using nanocrystals, including scalable synthesis of high-performance nanocrystals, nanocrystal surface oxidation during printing processes, and poor density and electrical conductivity of the printed films<sup>20</sup>.

Here, we report a study of flexible thermoelectric films by screen printing colloidal inks composed of bismuth telluride based nanoplates fabricated using a scalable microwave-stimulated wet chemical approach<sup>21</sup> (shown in Fig. 1). The peak ZT of our flexible films reaches 0.43 at 175 °C due to a combination of high power factor and low thermal conductivity, which is among the highest ZT reported for flexible thermoelectric materials fabricated by printing. The films demonstrate superior flexibility with negligible changes in electric resistance with 150 bending cycles. In addition to the unprecedented high ZT and flexibility, another significant advantage of our work is the use of thioglycolic acid (TGA) as a surface capping agent to inhibit nanocrystal oxidation<sup>21</sup>, thus enabling large-scale manufacturing at ambient conditions.

## Methods

**Nanocrystal ink synthesis.** Our doped and functionalized pnictogen chalcogenide nanocrystals of  $\text{Bi}_2\text{Te}_{2.8}\text{Se}_{0.2}$  were synthesized using a microwave stimulated wet-chemical synthesis method based on inexpensive organic solvents and metal salts described earlier<sup>21</sup>. In this method, the reaction between molecularly ligated chalcogen and pnictogen complexes was activated by microwave stimulation with the presence of thioglycolic acid (TGA), which serves as a shape-directing, oxide-inhibiting and sulfur-dopant delivery agent. The resulting precipitate is cleaned and dried in ambient conditions to obtain powders consisting of single-crystal nanoplates of 5- to 20-nm-thickness with bounding edge dimensions ranging between 50 to 500 nm.

The dried nanocrystals with the TGA capping agent were mixed with solvent and binder to produce viscous and thixotropic inks for screen printing. The optimized ink contains 58 wt.%  $\text{Bi}_2\text{Se}_{2.8}\text{Se}_{0.2}$  nanopowders, 39 wt.% Solvent ( $\alpha$ -Terpineol, from Sigma-Aldrich), 2 wt.% Binder (Disperbyk-110, from BYK U.S.A. Inc.), 1 wt.% Glass Frits (from Artglass Supplies, 325 mesh). The ink is thoroughly mixed using a planetary centrifugal mixer for 20 minutes followed by a vortex mixer for 10 minutes to get a uniform mixture.

**Flexible film fabrication.** As-prepared ink is screen printed on flexible polyimide substrates. The thermoelectric films of various thicknesses in the range of 10–100  $\mu\text{m}$  were obtained by controlling the screen mesh size and the number of repeated print passes. The printed films were first dried in air at 200 °C on a hot plate to remove the solvent and binder, followed by a cold compaction using a hydraulic press to consolidate the films. The film was finally sintered at 430 °C for 45 minutes in vacuum in order to remove the TGA surfactant and further improve the film density. The sintering temperatures are kept below the melting point of the polyimide substrate, though better thermoelectric properties could be obtained at higher sintering temperatures.

**Thermoelectric property measurement.** The temperature-dependent in-plane electrical conductivity and Seebeck coefficient of the film sample were measured simultaneously using a commercial Linseis Seebeck and resistivity instrument. The above two properties of the same sample were also measured using a home-built testing system, and the two sets of measurement results are within 2%. In order to measure the thermal conductivity of the sample, a freestanding film of about 100  $\mu\text{m}$  thickness was prepared under the same conditions as those for preparing thinner films on substrate. The temperature-dependent cross-plane thermal diffusivity of the freestanding film was measured using a laser flash instrument. The cross-plane thermal conductivity was then determined using the sample density measured using Archimedes method and the specific heat measured

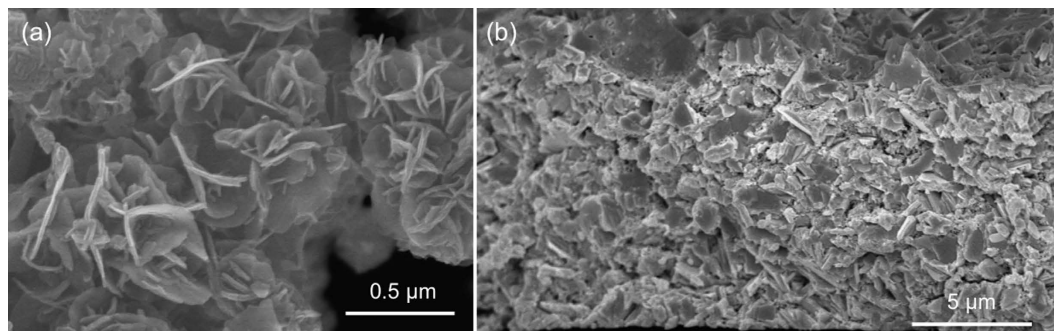


**Figure 2.** SEM images of (a) the  $\text{Bi}_2\text{Te}_{2.8}\text{Se}_{0.2}$  nanocrystals and (b) the cross section of a printed film on polyimide substrate.

using a DSC instrument. The in-plane thermal conductivity of the freestanding film was measured directly using a steady-state method in vacuum, which is within 5% of the cross-plane thermal conductivity, indicating the sample is isotropic. Details about the thermal conductivity measurement are included in the supplementary information. The carrier concentration and mobility were measured using Hall measurement conducted on the Physical Property Measurement System (PPMS) with 4 wire connection and the magnetic field sweeping from  $-1$  T to  $1$  T.

**Thermoelectric device fabrication and testing.** Five  $10\text{ mm} \times 2\text{ mm} \times 0.01\text{ mm}$  n-type  $\text{Bi}_2\text{Te}_{2.8}\text{Se}_{0.2}$  elements were printed onto a flexible polyimide substrate with  $4\text{ mm}$  spacing. Thin copper foils were soldered to the five elements in order to connect them electrically in series. A custom test bed was built using two commercial Peltier modules, one operating as a heater and the other as a cooler. The hot side and cold side of the TE device were thermally grounded to the two Peltier modules to create a temperature gradient. Two  $75\text{ }\mu\text{m}$  diameter k-type thermocouples were mounted to the hot and cold sides of the device to measure the temperature difference. The device was connected electrically in series with a shunt resistor and a variable resistor for impedance matching at each measurement temperature. The open circuit voltage, load voltage, current, internal resistance, and power output from the device were measured at each hot-side temperature while the cold-side temperature is maintained constant.

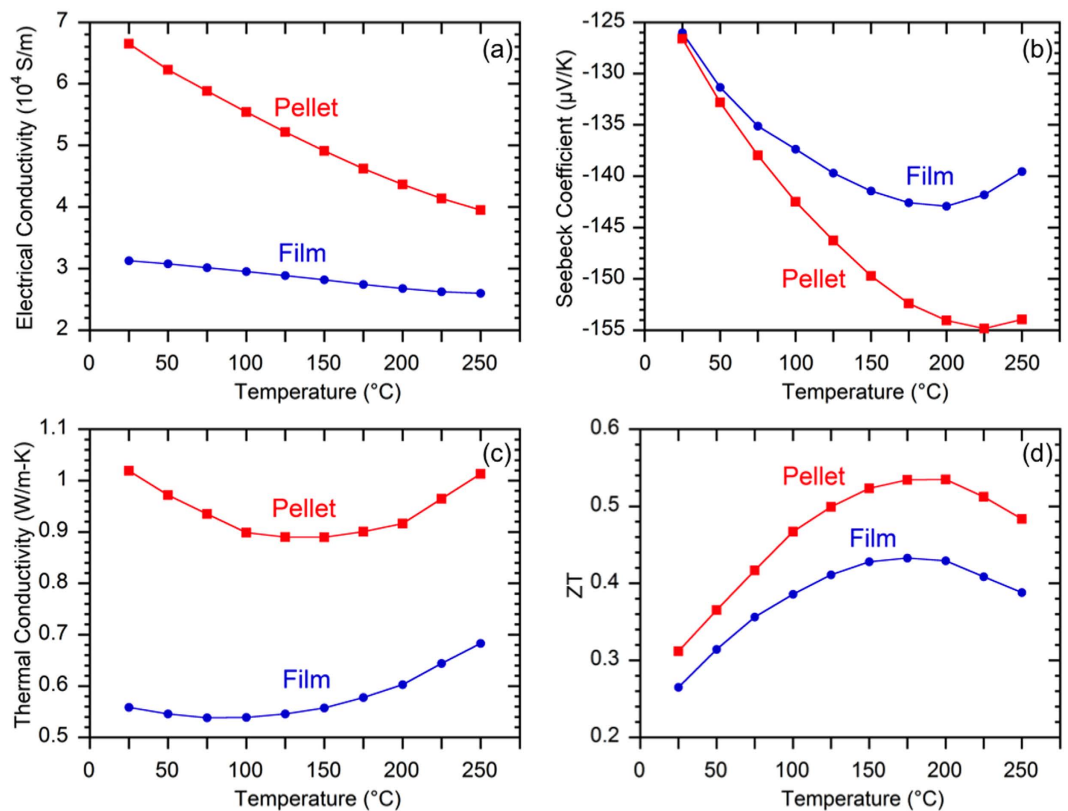
## Results and discussion

Figure 2(a) shows scanning electron microscope (SEM) images of the  $\text{Bi}_2\text{Te}_{2.8}\text{Se}_{0.2}$  nanocrystals, indicating the plate-like structures of several tens of nanometers thickness. Figure 2(b) shows a cross-section SEM image of a flexible  $\text{Bi}_2\text{Te}_{2.8}\text{Se}_{0.2}$  film of about  $10\text{ }\mu\text{m}$  thickness fabricated by screen printing. The films have about 85% relative density, and contain nanoscale pores primarily due to incomplete sintering of the nanocrystals and the removal of the additives in the ink.

Temperature-dependent thermoelectric properties were obtained on a flexible film of  $10\text{ }\mu\text{m}$  thickness printed using the nanocrystal ink and a reference pellet sample of  $500\text{ }\mu\text{m}$  thickness made by the pure nanocrystal powders using cold compaction and sintering under the same conditions. The relative densities of the film and the pellet are 85% and 90% respectively. As shown in Fig. 3(a), the room-temperature electrical conductivity of the film is about 53% lower than the pellet. Figure 3(b) shows the Seebeck coefficients of the two samples are within 10% for the entire measurement temperature, indicating approximately the same carrier concentrations for both the film and the pellet. Indeed, the Hall measurement validated that the carrier concentrations of the film and the pellet are within 10% ( $1.56 \times 10^{19}\text{ cm}^{-3}$  versus  $1.42 \times 10^{19}\text{ cm}^{-3}$ ), whereas the film mobility is about 56% lower than the pellet mobility ( $127\text{ cm}^2\text{V}^{-1}\text{s}^{-1}$  versus  $290\text{ cm}^2\text{V}^{-1}\text{s}^{-1}$ ) due to increased electron scattering by impurities and porosity present in the printed films.

The room-temperature lattice thermal conductivity  $\kappa_L$  of the film and the pellet is estimated to be  $0.41\text{ Wm}^{-1}\text{K}^{-1}$  and  $0.66\text{ Wm}^{-1}\text{K}^{-1}$ , respectively, using the equation  $\kappa_L = \kappa - \sigma TL$ , where  $\kappa$  is the total thermal conductivity,  $\sigma$  is the electrical conductivity,  $T$  is the absolute temperature, and  $L$  is the Lorenz number determined from our previous work<sup>22</sup>. The  $\kappa_L$  of these samples is significantly lower than their bulk counterpart attributed to the nanoscale grains and porosities originated from the nanocrystals<sup>22</sup>. Furthermore, the  $\kappa_L$  of the film is lower than the pellet mainly due to additional phonon defects scattering caused by the addition of glass particles as well as a small contribution from slightly higher porosities.

As shown in Fig. 3d, the film demonstrates a peak ZT of 0.43 at  $175\text{ }^\circ\text{C}$ , which is only 20% lower than control pellet despite 53% lower electrical conductivity. The significantly reduced thermal conductivity largely compensates the electrical conductivity losses and contributes to the high ZT in the printed films. In comparison, Table 1 summarizes the peak ZT (or room-temperature ZT if peak ZT is not available) of several representative n-type flexible thermoelectric materials, summarizing the highest reported ZT thus far in each category. The peak ZT of our flexible film is significantly higher than the previously reported bismuth telluride materials fabricated by printing, and is also among the highest reported value in all the reported n-type flexible thermoelectric films.



**Figure 3.** Temperature-dependent (a) Electrical conductivity (b) Seebeck coefficient (c) Thermal conductivity and (d) ZT of a 10  $\mu$ m thick flexible film fabricated by printing the nanoplate ink and a 500  $\mu$ m thick reference pellet fabricated by cold-compaction and sintering of the pure nanoplate powders.

Materials details	Power factor ( $\text{mWm}^{-1}\text{K}^{-2}$ )	Peak/room T' ZT	Ref.	Fabrication methods
$\text{Bi}_2\text{Te}_{2.8}\text{Se}_{0.2}$	0.56	0.43	(Ours)	Screen printing
$\text{Bi}_2\text{Te}_3$	1.33	0.35*	16	Screen printing
$\text{Bi}_2\text{Te}_3$ + Epoxy	0.28	0.31*	15	Dispenser printing
CNT	0.15	N.A.	23	Drop casting
$\text{WS}_2$	0.007	N.A.	24	Vacuum filtration
$\text{TiS}_2$ -Polymer	0.45	0.28	25	Electrochemical intercalation
CNT-PEDOT-TDAE	1.05	~0.5*	26	Spraying and spin coating

**Table 1.** The thermoelectric performance comparison between our work and previous reported n-type flexible thermoelectric films.

In order to test the flexibility, the room-temperature electrical resistance of the printed films was tested using Van der Pauw method as a function of bending cycles on two cylinders of 7 mm radius and 5 mm radius respectively. Electrical resistance is chosen here to evaluate film flexibility because it is very sensitive to any cracks that may develop during bending test. After 150 bending cycles, the electrical resistances of the film show 1.4% increase for the 7 mm bending radius and 4.5% increase for the 5 mm bending radius respectively, indicating superior bending flexibility (shown in Fig. 4).

A thermoelectric generator device consisting of 5 n-type elements (shown in Fig. 5(a) inset) was fabricated in order to validate the performance of the flexible films. Figure 5 shows the experimental and simulation results of the device tested at different temperature differences ( $\Delta T$ ) when the hot side temperature was varying from 40–80 °C and the cold side was maintained at 20 °C. The open circuit voltage, device voltage during operation, and power output increase as the  $\Delta T$  increases. As shown in Fig. 5(a,c), the maximum open circuit voltage and power density reach 41 mV and 4.1  $\text{mW}/\text{cm}^2$  with 60 °C  $\Delta T$ . The power density was determined based on the total cross-sectional area (2 mm  $\times$  0.01 mm  $\times$  5) of the five thermoelectric elements. The experimental results are within 10% of the finite element simulation results based on the thermoelectric properties shown in Fig. 3, which further verified the measured film properties. Figure 5(b,d) shows the device operating voltage and power output as a function of electrical current tested by varying the external load resistances.

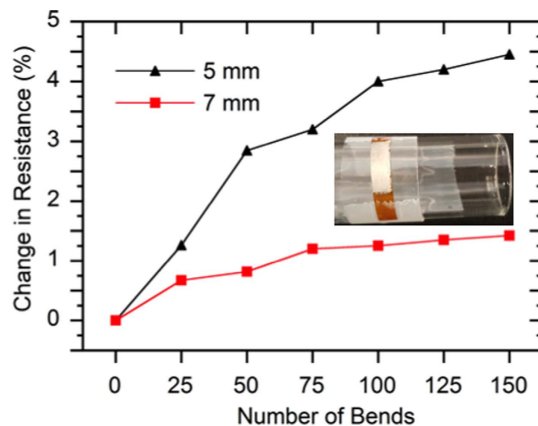


**Figure 4.** Percentage increase of electrical resistances of flexible films as a function of number of bending cycles for 7 mm bending radius and 5 mm bending radius.

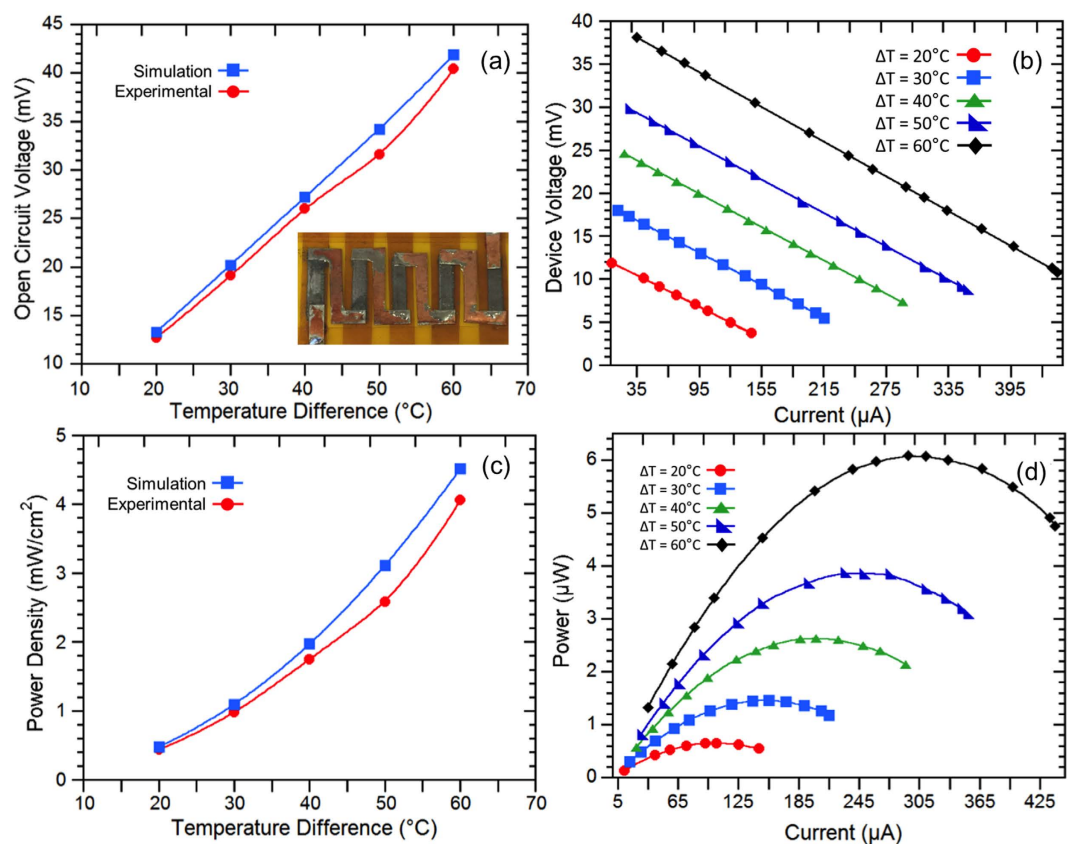


**Figure 5.** Testing results of a thermoelectric device fabricated by the screen printed flexible films. (a) Experimental and calculated open circuit voltage vs. temperature differences ( $\Delta T$ ), (b) Device operating voltage vs. current tested at various  $\Delta T$ , (c) Experimental and calculated electrical power density vs.  $\Delta T$  (d) Electrical power output tested at various  $\Delta T$ . Inset in (a) is a picture of the device.

The maximum power of  $6.1 \mu\text{W}$  is obtained with  $60^\circ\text{C}$   $\Delta T$  when the external load resistance matches with the internal resistance of the device.

## Conclusions

Flexible thermoelectric films were screen printed at ambient conditions using nanocrystals synthesized by a highly scalable microwave assisted wet chemical method. The films show an unprecedented peak ZT of 0.43 at  $175^\circ\text{C}$  and superior flexibility with negligible changes of electrical conductivity after 150 bending cycles. The flexible thermoelectric device fabricated using the printed n-type thermoelectric elements produces a high power density of  $4.1 \text{ mW}/\text{cm}^2$  with a small temperature difference of  $60^\circ\text{C}$ , opening up lots of applications for

low-temperature energy harvesting. The performance of the printed thermoelectric films and devices can be further improved by increasing the electrical conductivity through optimization of the ink formulation and refinement of the sintering process.

## References

- Rowe, D. M. *Thermoelectrics handbook: macro to nano*. 5–10 (CRC/Taylor & Francis, 2006).
- Bahk, J.-H., Fang, H., Yazawa, K. & Shakouri, A. Flexible thermoelectric materials and device optimization for wearable energy harvesting. *J Mater Chem C* **3**, 10362–10374 (2015).
- Goldsmid, H. J. *Thermoelectric refrigeration*. 240–241 (Plenum Press, 1964).
- Rowe, D. M. *CRC handbook of thermoelectrics*. 701–702 (CRC Press, 1995).
- Dresselhaus, M. S. *et al.* New directions for low-dimensional thermoelectric materials. *Adv Mater* **19**(8), 1043–1053 (2007).
- Hicks, L. D. & Dresselhaus, M. S. Effect of Quantum-Well Structures on the Thermoelectric Figure of Merit. *Phys Rev B* **47**(19), 12727–12731 (1993).
- Snyder, G. J. & Toberer, E. S. Complex thermoelectric materials. *Nat Mater* **7**(2), 105–114 (2008).
- Minnich, A. J., Dresselhaus, M. S., Ren, Z. F. & Chen, G. Bulk nanostructured thermoelectric materials: current research and future prospects. *Energ Environ Sci* **2**(5), 466–479 (2009).
- Shakouri, A. Recent developments in semiconductor thermoelectric physics and materials. *Annual Rev Mater Res* **41**, 399–431 (2011).
- Zhao, L. D., Dravid, V. P. & Kanatzidis, M. G. The panoramic approach to high performance thermoelectrics. *Energ Environ Sci* **7**(1), 251–268 (2014).
- Yee, S. K., LeBlanc, S., Goodson, K. E. & Dames, C. \$ per W metrics for thermoelectric power generation: beyond ZT. *Energ Environ Sci* **6**(9), 2561–2571 (2013).
- Jiao, F. *et al.* Inkjet-printed flexible organic thin-film thermoelectric devices based on p- and n-type poly(metal 1,1,2,2-ethenetetrathiolate)/polymer composites through ball-milling. *Philos Trans A Math Phys Eng Sci* **372**, 20130008 (1–10) (2014).
- Koplow, M., Chen, A., Steingart, D., Wright, P. K. & Evans, J. W. In *Thick film thermoelectric energy harvesting systems for biomedical applications*, Medical Devices and Biosensors, 2008. ISSS-MDBS 2008. 5th International Summer School and Symposium on, 1–3 June 2008; pp 322–325 (2008).
- Lu, Z. Y. *et al.* Fabrication of flexible thermoelectric thin film devices by inkjet printing. *Small* **10**(17), 3551–3554 (2014).
- Madan, D. *et al.* Enhanced performance of dispenser printed MA n-type Bi<sub>2</sub>Te<sub>3</sub> composite thermoelectric generators. *ACS Appl Mater Inter* **4**(11), 6117–6124 (2012).
- Kim, S. J., We, J. H. & Cho, B. J. A wearable thermoelectric generator fabricated on a glass fabric. *Energ Environ Sci* **7**(6), 1959–1965 (2014).
- Kim, S. J., We, J. H., Kim, J. S., Kim, G. S. & Cho, B. J. Thermoelectric properties of P-type Sb<sub>2</sub>Te<sub>3</sub> thick film processed by a screen-printing technique and a subsequent annealing process. *J Alloys Compounds* **582**, 177–180 (2014).
- Lee, H. B. *et al.* Thin-film thermoelectric module for power generator applications using a screen-printing method. *J Electronic Mater* **40**(5), 615–619 (2011).
- We, J. H., Kim, S. J., Kim, G. S. & Cho, B. J. Improvement of thermoelectric properties of screen-printed Bi<sub>2</sub>Te<sub>3</sub> thick film by optimization of the annealing process. *J Alloys Compounds* **552**, 107–110 (2013).
- Kamyshny, A. & Magdassi, S. Conductive nanomaterials for printed electronics. *Small* **10**(17), 3515–3535 (2014).
- Mehta, R. J. *et al.* A new class of doped nanobulk high-figure-of-merit thermoelectrics by scalable bottom-up assembly. *Nat Mater* **11**(3), 233–240 (2012).
- Zhang, Y. *et al.* Lattice thermal conductivity diminution and high thermoelectric power factor retention in nanoporous macroassemblies of sulfur-doped bismuth telluride nanocrystals. *Appl. Phys. Lett.* **100**(19), 193113 (2012).
- Yu, C. H., Murali, A., Choi, K. W. & Ryu, Y. Air-stable fabric thermoelectric modules made of N- and P-type carbon nanotubes. *Energ Environ Sci* **5**(11), 9481–9486 (2012).
- Oh, J. Y. *et al.* Chemically exfoliated transition metal dichalcogenide nanosheet-based wearable thermoelectric generators. *Energ Environ. Sci.* **9**, 1696–1705 (2016).
- Wan, C. L. *et al.* Flexible n-type thermoelectric materials by organic intercalation of layered transition metal dichalcogenide TiS<sub>2</sub>. *Nat Mater* **14**(6), 622–627 (2015).
- Wang, H. *et al.* Thermally driven large N-Type voltage responses from hybrids of carbon nanotubes and poly(3,4-ethylenedioxythiophene) with tetrakis(dimethylamino) ethylene. *Adv Mater* **27**(43), 6855–6861 (2015).

## Acknowledgements

This work is funded by the US Department of Energy, Office of Nuclear Energy, under Award number DE-NE0008255. C.H. acknowledges financial support from US NSF fellowship support. N.K. acknowledges financial support from US DOE NEUP fellowship support. The authors thank Luke Schoensee for graphical support on this work.

## Author Contributions

T.V. fabricated the flexible films. C.H. and N.K. carried out thermoelectric property measurements. J.R. fabricated and tested the thermoelectric device. P.G. carried out simulation of the TEG device. C.H. performed SEM characterizations. D.E. and R.J.M. contributed to the ideas and discussions of this work. Y.Z. is the principle investigator who devised and supervised this work. All the authors contributed to the writings of the manuscript.

## Additional Information

**Supplementary information** accompanies this paper at <http://www.nature.com/srep>

**Competing financial interests:** The authors declare no competing financial interests.

**How to cite this article:** Varghese, T. *et al.* High-performance and flexible thermoelectric films by screen printing solution-processed nanoplate crystals. *Sci. Rep.* **6**, 33135; doi: 10.1038/srep33135 (2016).



This work is licensed under a Creative Commons Attribution 4.0 International License. The images or other third party material in this article are included in the article's Creative Commons license, unless indicated otherwise in the credit line; if the material is not included under the Creative Commons license, users will need to obtain permission from the license holder to reproduce the material. To view a copy of this license, visit <http://creativecommons.org/licenses/by/4.0/>